



RESEARCH ARTICLE

Electrochemical Detection of Hydrazine Pesticide with Fe₂O₃ NanoparticlesNeelam¹, Gita Rani*¹ and Mukesh Kumar²¹Department of Chemistry, Chaudhary Devi Lal University, Sirsa, India²Department of Education, AMSSS Jhiri, Sirsa, India

*Email: gtcdlu@gmail.com

Received: 23rd March 2017, Revised: 21st May 2017, Accepted: 24nd May 2017

ABSTRACT

In this work we present the application of multiwalled carbon nanotubes (MWCNTs) paste electrode modified with iron oxide nanoparticles for the detection of hydrazine pesticide in food and vegetables. The synthesized nanoparticles was characterized by scanning electron microscopy (SEM), fourier transform infrared spectroscopy (FTIR), X-ray diffraction (XRD), energy-dispersive X-ray spectroscopy (EDX). The electrochemical studies were carried out by cyclic voltammetry and chronoamperometry with the help of three electrode autolab system. The electrooxidation behavior of Fe₂O₃/MWCNT SPCE showed optimal response (<5s), good sensitivity (61.76 $\mu\text{A } \mu\text{M}^{-1} \text{cm}^{-2}$) and low detection limit 5 μM and long term stability.

Key words: Iron oxide nanoparticles, Co-precipitation method, XRD, SEM, hydrazine.

INTRODUCTION

Hydrazine (NH₂NH₂) is an insecticide pesticide used in agricultural and also used as fuel for rockets. It is used for missiles and satellite in aerospace, military field, metal film manufactures and photographic chemicals (Trojan, 1953). Hydrazine also has hepatotoxic and carcinogenic effects and can be absorbed through skin, causes kidney and liver damages (Toth, 1988). Therefore its determination is very important. There are several methods available for the detection of hydrazine pesticide like chromatography (Kirchherr, 1993), titrimetry (Budkuley, 1992), amperometry (Wyatt, *et. al.* 1993), potentiometry (Singh, *et. al.* 1996), spectrophotometry (Safavi, *et. al.* 1995) and coulometry (Pastor, *et. al.* 1983). Carbon based materials like multiwalled carbon nanotubes (MWCNT) play an important role in the development of sensor (Yang, *et. al.* 2017, Zeng, *et. al.* 2016). Electrochemical biosensor based on metal nanoparticles, carbon nanotube and graphene have been reported for the determination of hydrazine (Devasenathipathy, *et. al.* 2014, Karimi, *et. al.* 2014, Zhao, *et. al.* 2016).

In this paper, we synthesized iron oxide nanoparticles by coprecipitation method and fabricate working electrode by modified with iron oxide and multiwalled carbon nanotube over screen printed electrode. In order to test the electrochemical sensing of Fe₂O₃/MWCNT electrode we investigated the oxidation of hydrazine as an electroactive species. We have found that Fe₂O₃/MWCNT modified screen printed electrode presents a good sensitivity towards the hydrazine detection in food samples.

EXPERIMENTAL

Materials:

Ferrous sulphate heptahydrate (FeSO₄ 7H₂O) was purchased from central drug house. Potassium chloride (KCl), multiwalled carbon nanotube (MWCNT) were purchased from CDH, New Delhi. All others chemicals were of analytical grade and used without further purification. The stock solutions of hydrazine were freshly prepared in phosphate buffer (pH 7.0).

Synthesis of Fe₂O₃ Nanoparticles:

Fe₂O₃ nanoparticles were prepared by coprecipitation method. In this method, 0.1 M FeSO₄ 7H₂O solution were prepared in double de-ionized water with continuous stirring to get a

homogeneous solution. 0.1 M sodium hydroxide solution was added dropwise into the above solution with continuous stirring for 3 hrs. The resultant precipitates thus obtained were washed with double distilled water and after acetone. Precipitates were dried at 100°C in oven for 5 hrs. Finally these were put into muffle furnace at 600°C for 2 hrs and iron oxide nanoparticles were formed.

Fabrication of Fe₂O₃/CNT Modified Screen Printed Carbon Electrode:

Carbon nanotubes (CNT), nanoparticles (NP) and gluteraldehyde were prepared by mixing in the ratio 5:3:2. Mix the above solution vigorously to get a homogeneous mixture. The above solution was then used for the fabrication process of the screen printed carbon electrode. The dot of SPCE i.e. working electrode was filled with above slurry using the pipette. Then the electrode was dried in the microwave oven at 70°C for 5 minutes and left at room temperature for 24 hrs for the fixation of slurry on the working electrode dot of SPCE.

Characterization:

The crystalline size of Fe₂O₃ nanoparticles was investigated by using X-ray diffraction (XRD) pattern, using D-8 Advance, Bruker diffraction, with monochromatic Cu K α radiation ($\lambda = 1.5418 \text{ \AA}$). Scanning electron microscope (SEM) analysis was done through Hitachi S3700 SEM using an acceleration of 15 KV. The size of nanoparticles are calculated by SEM. The cyclic voltammetry (CV) and chronoamperometry (CA) studies have been done using an Autolab Potentiostat/Galvanostat (Metrohm). The electrochemical measurements have been conducted on a three-electrode system using Fe₂O₃/CNT/SPCE as the working electrode, a platinum (Pt) wire as the counter and saturated Ag/AgCl as a reference electrode in a phosphate buffer saline (PBS, pH 7.0, NaCl) containing 5 mM [Fe(CN)₆]^{3-/4-} as a mediator.

RESULT AND DISCUSSION

FTIR Analysis:

The FTIR spectra of iron oxide nanoparticles were synthesized by co-precipitation method. The strong and sharp absorption peak at 562 cm⁻¹ and 445.5 cm⁻¹ corresponds to the Fe-O stretching and bending modes of Fe₂O₃ nanoparticles respectively. Broad absorption peak above 3400 cm⁻¹ stands for the O-H bond in the hydroxyl group.

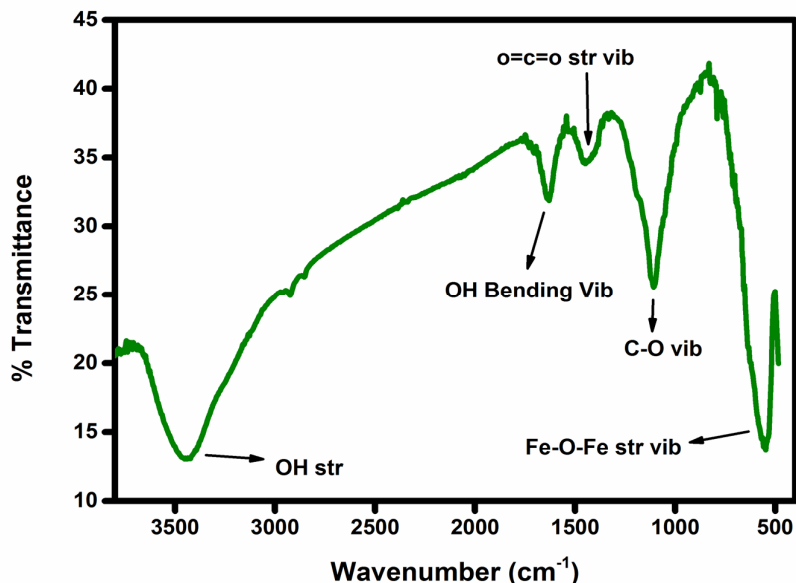


Fig. 1: FTIR spectra of iron oxide NPs

SEM Analysis:

The surface morphology of synthesized iron oxide NPs shows the magnification of 5.00 μm . The iron oxide nanoparticles are crystalline in nature and 20-70 nm in size.

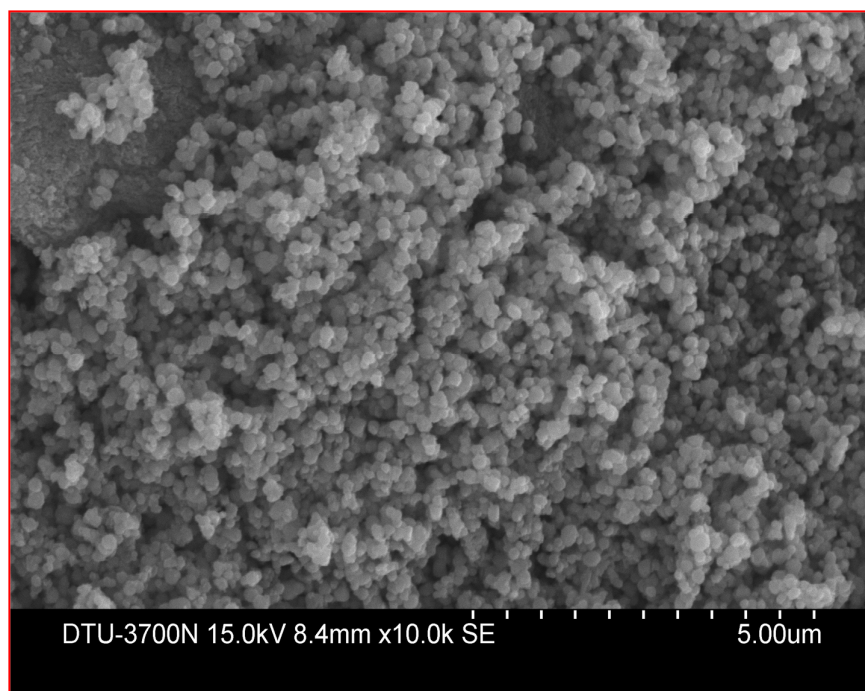


Fig. 2: SEM image of iron oxide NPs

XRD Spectra:

Figure 3 shows the XRD of iron oxide nanoparticles. By comparing the XRD pattern with the JCPDS card file 39-1346, the characteristic peaks are observed at 2θ angle 33.210, 35.450, 44.560, 57.450, 62.550 which corresponds to the Bragg reflection (104), (110), (202), (122), (214) respectively. The particle size of synthesized iron oxide NPs was found to be 66.0nm by using scherrer's formula $d = K\lambda/\beta\cos\theta$. Where the constant K is taken to be 0.94, λ is the wavelength of X-ray, β is the full width at half maximum and θ is the half of Bragg angle.

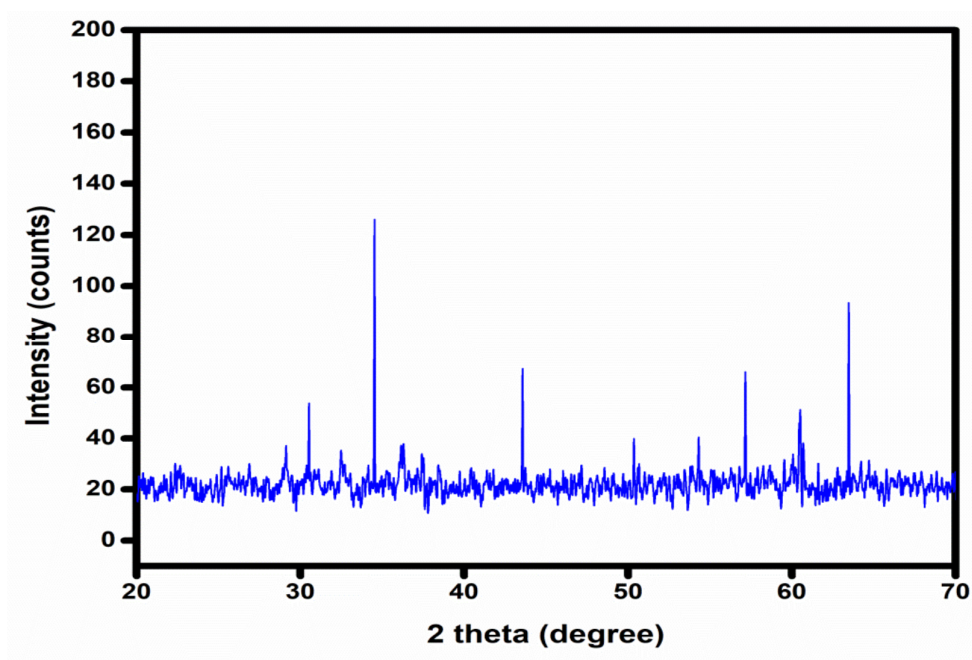


Fig. 3: XRD spectra of iron oxide NPs

EDX Spectra:

Figure 4 shows the EDX spectra of iron oxide nanoparticles synthesized by co-precipitation method. The energy dispersive X-ray spectrometry (EDX) analysis was used to know the molecular ratio of iron and oxygen in the synthesized Fe_3O_4 NPs. The EDX spectrum of Fe_3O_4 contains iron and oxygen elements in atomic percentage are found to be 53.49% and 46.51% respectively in the sample.

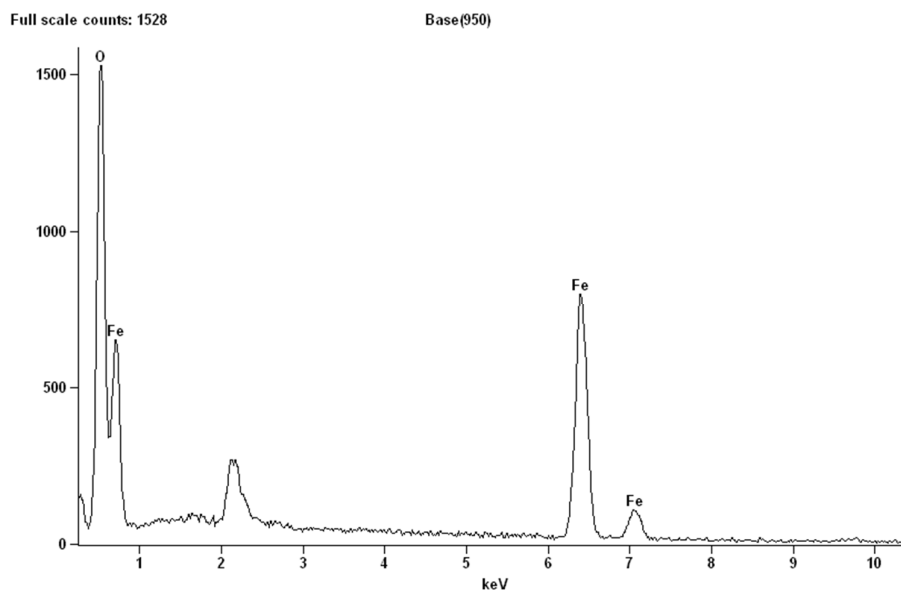


Fig. 4: EDX spectra of iron oxide NPs

ELECTROCHEMICAL STUDIES**Cyclic Voltammetry:**

Figure 5 (a) showed the cyclic voltammograms of 0.5 mM hydrazine in 0.1 M PBS (pH 7.0) measured on $\text{Fe}_2\text{O}_3/\text{CNT}$ modified SPCE. After modification it exhibited the higher anodic peak current than the unmodified SPCE. The oxidation peak appeared at 792 mV with an I_{pa} value of 790 μA . The observed modified CV graph is responsive towards hydrazine. In figure 5 (b) the scan rate experiments were also performed in 0.1 M PBS (pH 7.0) containing 0.5 mM hydrazine at the different scan rates in a range of 5, 10, 20, 50 and 100 mVs^{-1} . The observed scan rate dependent CV graph represents that the increase in the scan rate, current values also increases which shows that the oxidation process is diffusion controlled. In figure 5 (b) linear relationship is observed between anodic current (I_{pa}) and $v^{1/2}$, which proves the diffusion-controlled kinetics. According to Randles-Sevcik equation the number of electrons is 2.

Chronoamperometry:

Amperometric experiments were performed using the $\text{Fe}_2\text{O}_3/\text{CNT}$ modified SPCE. Figure 6 (a) shows the response of the modified SPCE on the successive addition of hydrazine i.e 5, 10, 15, 20, 25, 30, 35, 40, 45 and 50 μM in 0.1 M PBS (pH 7.0) solution at constant potential of 0.45 V. The fabricated sensor shows the current response increase after the addition of hydrazine. Figure 5.4.2 (b) depicts the plot between current vs hydrazine concentration. From the graph it is clear that with increase the concentration of hydrazine the value of current increases and that greatly shows the linear relationship. The sensitivity of the fabricated hydrazine sensor was 61.76 $\mu\text{A } \mu\text{M}^{-1} \text{ cm}^{-2}$. The relationship between the hydrazine concentration and anodic peak current showed a linear regression of $I_{pa} (\mu\text{A}) = 15.44 (\mu\text{M}) + 5.33$ with correlation coefficient (R^2) of 0.996. The detection limit of fabricated hydrazine sensor was found to be 5 μM and the response time was <5 sec.

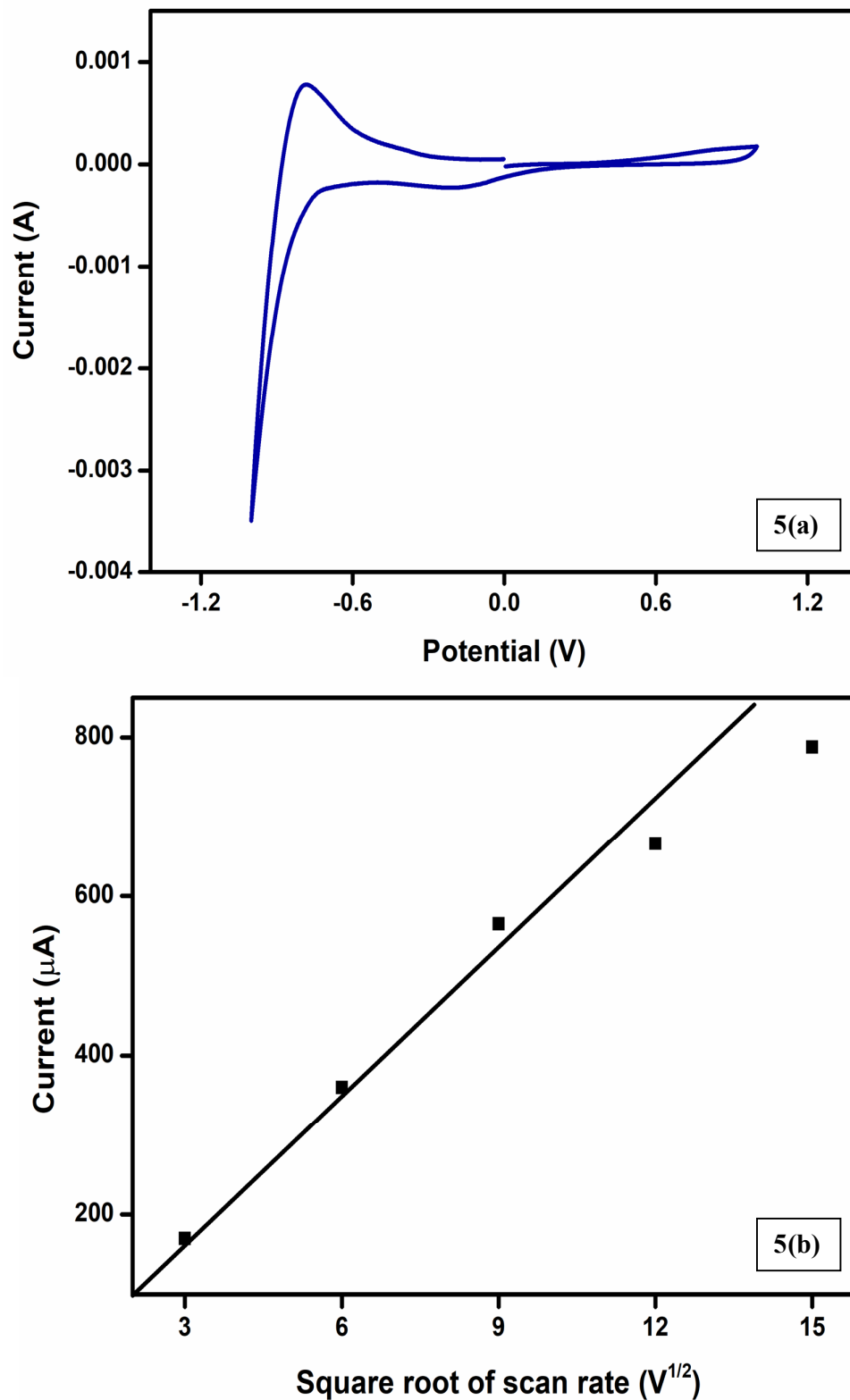


Fig. 5 (a): Cyclic Voltammograms of 0.5 mM hydrazine in 0.1 M PBS (pH 7.0) with scan rate of 100 mV/s obtained at modified SPCE **(b):** Different scan rates (5, 10, 20, 50, 100 mV/s) of modified electrode of 0.5 mM hydrazine in 0.1 M PBS.

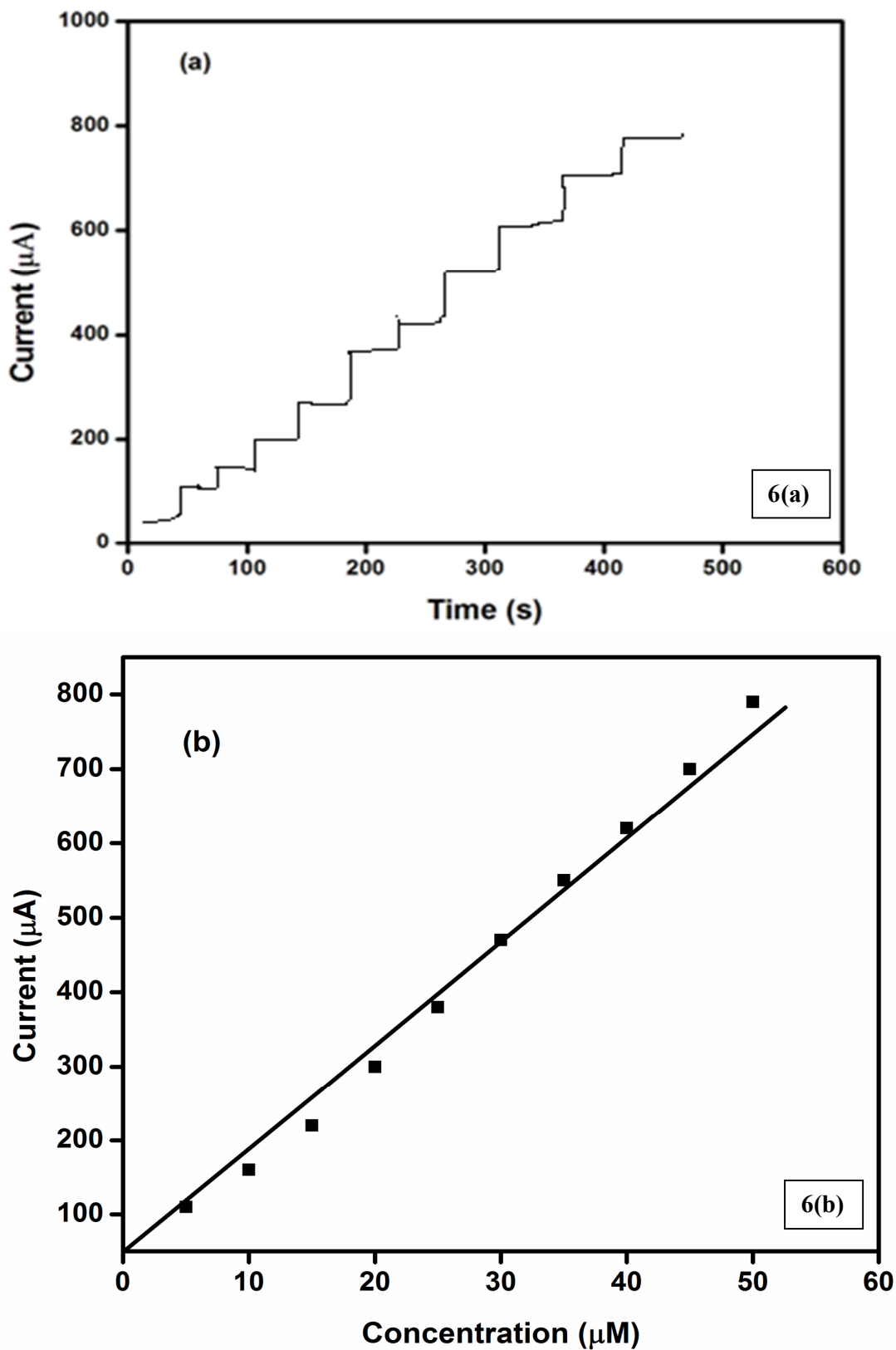


Fig 6(a): Chronoamperometry of modified SPCE with successive addition of hydrazine into 0.1 M PBS (pH 7.0) and **(b):** plot between current vs hydrazine concentrations.

CONCLUSION

The above synthesized nanoparticles were characterized by several techniques. The electrooxidation behavior of Fe₂O₃/MWCNT SPCE showed optimal response (<5s), good sensitivity (61.76 $\mu\text{A } \mu\text{M}^{-1} \text{ cm}^{-2}$) and low detection limit 5 μM and long term stability. This proposed electrode was used for rapid determination of hydrazine in food samples.

REFERENCES

1. Budkuley J. (1992): Determination of hydrazine and sulphite in the presence of one another. *Mikrochimica Acta*, Vol.108: 103–105.
2. Devasenathipathy R., et al. (2014): Highly selective amperometric sensor for the trace level detection of hydrazine at bismuth nanoparticles decorated graphene nanosheets modified electrode. *Talanta*, Vol. 124: 43-51.
3. Karimi H., et al. (2014): An electrochemical nanocomposite modified carbon paste electrode as a sensor for simultaneous determination of hydrazine and phenol in water and wastewater samples. *Environmental Science and Pollution Research*, 21: 5879-5888.
4. Kirchherr H. (1993): Determination of hydrazine in human plasma by high-performance liquid chromatography. *Journal of Chromatography B: Biomedical Science Applied*, Vol.617: 157–162.
5. Pastor T., et al. (1983): Coulometric determination of thiols and hydrazines with electro generated iodine in methanol in the presence of potassium acetate. *Mikrochimica Acta*, Vol. 81: 203–211.
6. Safavi A., et al. (1995): Kinetic spectrophotometric determination of hydrazine. *Analytica Chimica Acta*, Vol. 300: 307–311.
7. Singh N.S.B., et al. (1996): A new potentiometric determination of hydrazine in the presence of uranium(IV). *Journal of Radioanalytical Nuclear Chemistry*, Vol. 209: 211–215.
8. Toth B. (1988): Toxicities of hydrazines: a review, *In Vivo*, 2: 209-242.
9. Troyan J.E. (1953): Properties, production and uses of hydrazine. *Industrial and Engineering Chemistry*, Vol. 45: 2608-2612.
10. Wyatt J.R., et al. (1993): Coulometric method for the quantification of low-level concentrations of hydrazine and mono methyl hydrazine. *American Industrial Hygiene Association Journal*, Vol. 54: 285–292.
11. Yang Y.J., et al. (2017): Immobilization of phosphor tungstic acid on multiwalled carbon nanotubes with cetyltrimethyl ammonium bromide as the molecular linker for enhanced oxidation of hydroxylamine. *Journal of Electroanalytical Chemistry*, Vol. 799: 386-392.
12. Zeng Y., et al. (2016): Nanomaterial-based electrochemical biosensors for food safety. *Journal of Electroanalytical Chemistry*, Vol. 781: 147-154.
13. Zhao Z.T., et al. (2016): Preparation and characterization of AuNPs/CNTs-ErGO electrochemical sensors for highly sensitive detection of hydrazine. *Talanta*, Vol. 158: 283-291.